The Structure and Motion of Severe Hailstorms. Part II: Multi-Cell Storms[1]

JOHN D. MARWITZ[2]

Dept. of Meteorology, McGill University, Montreal, Canada

(Manuscript received 18 June 1971)

ABSTRACT

Two case studies are presented of multi-cell storms in Alberta which displayed separate modes of propagation. Discrete propagation occurred on the right flank of both storms as in multi-cell storms previously documented by Browning and Ludlam in England and Chisholm in Alberta. The storms which were synthesized by Browning and Ludlam and by Chisholm deviated to the right due only to discrete propagation. The individual cells of the first storm (Alhambra storm) propagated continuously to the right in addition to the discrete propagation, which caused the Alhambra storm to deviate ~55° to the right of the mean environmental winds. On the other hand, the individual cells in the second storm (Rimbey storm) were observed to propagate continuously to the left of the mean environmental winds. The continuous propagation of the cells to the left was offset by the discrete propagation to the right. Schematic models of the Wokingham, Alhambra and Rimbey storms are presented.

1. Introduction

The radar echo from the storm which occurred near Wokingham, England, on 9 July 1959 consisted of a series of aligned cells which individually moved with the mean environmental winds. New cells periodically developed on the right flank, moved with the storm complex, and finally dissipated on the left flank (Browning and Ludlam, 1960). This form of discrete propagation caused deviate motion toward the right flank. During the storm's most intense stage the deviate motion remained the same, although the PPI echo near cloud base height was uniform, i.e., individual cells could not be identified during the intense stage. Browning and Ludlam (1962) emphasized the intense stage during their second article on this storm, where they proposed a three-dimensional storm model which included continuous propagation on the right flank. We shall see in Section 3 that individual cells could not be identified near cloud base height in the Alhambra storm either, but they were identifiable near the top.

Chisholm (1966) synthesized two multi-cell storms which occurred in Alberta. Both storms deviated toward the right flank by discrete propagation while individual cells within the storm complex tended to move in the direction of the environmental winds.

The "feeder" cloud concept described by Dennis *et al.* (1970) also appears to be a form of the multi-cell concept first described by Browning and Ludlam (1960).

The University of Wyoming aircraft system was flown in the updrafts near cloud base of ~12 severe Alberta hailstorms during the months of July 1968, July 1969 and July 1970. The Alberta Hail Studies (ALHAS) radar obtained three-dimensional reflectivity data at 3-min intervals on each storm throughout its lifetime. Each storm was also surveyed for rain and hail by means of a unique telephone survey system. The data for eight of the above storms have been synthesized by the author, six of which could be identified as multi-cell storms. Of these six cases, only two will be presented; they were selected because they individually exhibited two additional modes of propagation rather different from the Wokingham storm and from Chisholm's (1966) storms.

2. Project area and observation systems

The ALHAS project area is shown in Fig. 1, with the radar, rawinsonde, aircraft and telephone survey crews being centrally located at Mynarski Park near Penhold, Alberta. The terrain features in Alberta are very similar to those of northeastern Colorado with the mountain peaks also ~150 km to the west-southwest and reaching 4.0 km, while those in the project area were ~1.0 km in height. The ALHAS project area is heavily forested in comparison to northeastern Colorado. The University of Wyoming aircraft system was described in Marwitz (1972).

The ALHAS radar was a modified AN/FPS-502 with the following characteristics:

[1] This paper has been abstracted from a Ph.D. thesis submitted to McGill University.

[2] Permanent affiliation: Department of Atmospheric Resources, Laramie, University of Wyoming.

Peak transmitted power	250 kW
Beamwidth	1.15°
Pulse length	525 m
Pulse repetition rate	480 sec^{-1}
Wavelength	10.4 cm
Antenna rotation rate	8 rpm

The antenna was operated by a programmed scan which spiraled the antenna from 0° to 20° at 1° per revolution. The spiral scan took 3 min. The returned power for each antenna revolution was displayed on a PPI scope at 10-dB discrete grey scale levels and recorded on 35-mm film. The grey scale levels were calibrated each day to ±2 dB.

3. The Alhambra storm of 12 July 1969

The aircraft departed from Penhold shortly after 1300 (all times MST) to study a storm occurring south of ALHAS. By 1400 another storm began to show visual and radar signs of intensifying. This new storm was ~80 km WNW of ALHAS and passed over Alhambra near 1445. Since the two storms were separated by > 150 km and a substantial amount of data had been gathered on the first storm, the air crew was understandably reluctant to leave this storm. Besides, there was no firm knowledge that the new storm would persist. After completing a series of measurements on the first storm, the aircraft was directed to the new storm and began observation at 1510.

The locations of this new storm and its reflectivity pattern near cloud base are shown at ~30-min intervals in Fig. 2. The trajectory of the storm was approximately S-shaped. Fankhauser (1967) and others have observed trajectories of this shape when studying Oklahoma storms. The horizontal velocity changed as the storm executed changes in direction. The velocity was 270° at 11 m sec^{-1} during the developing stage, changed to 300° at 9 m sec^{-1} during its most intense stage, and finally became 255° at 15 m sec^{-1} when the storm dissipated.

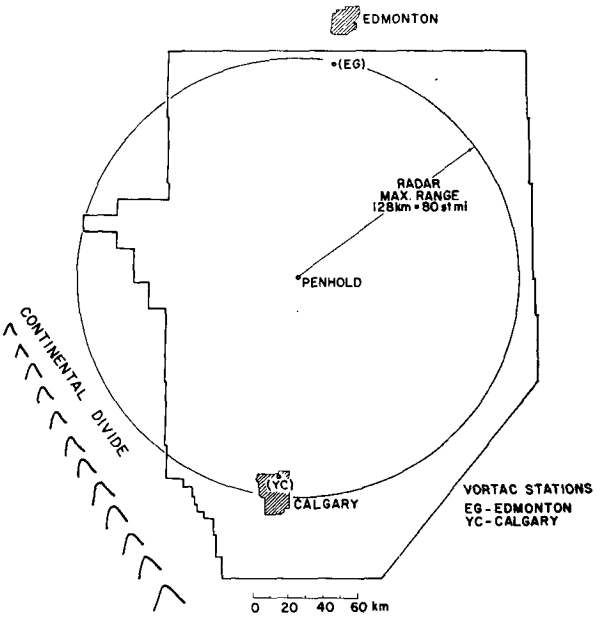

FIG. 1. Map of Alberta Hail Studies area in Alberta.

The hodograph of the rawinsonde winds obtained from Penhold at 1545 is shown in Fig. 3. The motions of the storm as obtained from the radar echo are plotted on this hodograph. The velocity of the storm decreased as the direction deviated farther to the right of the mean environmental winds. The motion of the storm deviated ~55° to the right of the mean environmental winds during the intermediate stage when, as we shall see in the next section, the storm was at its most intense stage.

The hailfall pattern is shown in Fig. 4. The envelope of the level three echo from the radar scan near cloud base is included for easier cross referencing to other figures. The areas within which hail ≥ grape size fell are also indicated. Almost all of the hail which reached the

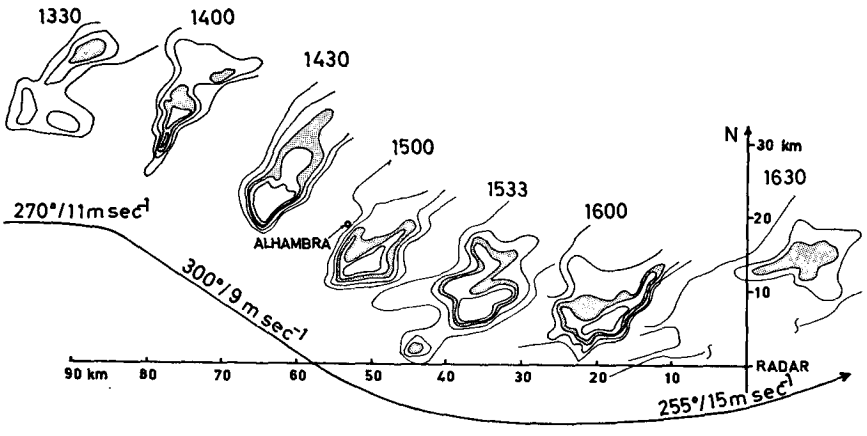

FIG. 2. Echo patterns near cloud base for the Alhambra storm of 12 July 1969. The outer edge of the shaded contour is level three, corresponding to 30 dBZ at 29 km.

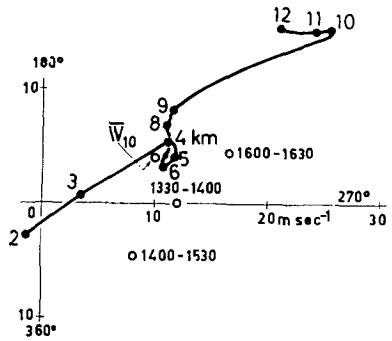

FIG. 3. Hodograph of Penhold rawinsonde winds for 12 July 1969. Storm motions are also included.

ground occurred while the storm was deviating toward the right. The largest hail fell during the greatest deviate motion and produced a hailswath oriented along the direction of motion of the radar echo.

It should be noted that the largest hail fell on the southwest side of the hailswath while rain and the smallest hail fell on the northeast side.

As was noted earlier, the aircraft arrived at this storm during the latter part of its most intense phase and then mapped the updraft at cloud base for ~1 hr. The flight track and observed updrafts are indicated in Fig. 5. During the first few passes prior to 1515 the area of the updrafts was estimated to be ~10 km in length along the leading edge of the storm and extended ~4 km in width ahead of the precipitation curtain. The updrafts averaged ~5 m sec^{-1} over this area (40 km^2). After 1515 the updrafts gradually decreased in magnitude and areal extent, while only small areas of weak updrafts were observed after 1545. By 1610 it was obvious to the air crew that this storm did not contain any organized updraft pattern, and the storm direction of motion had become aligned with the mean winds.

PPI echoes from four separate spiral scans are presented in Fig. 6. The first spiral scan (1333) shows the echo during its development and prior to the occurrence of deviate motion. The middle two spiral scans (1433 and 1509) were taken during the most intense phase of the storm, when it displayed the greatest deviate motion. The last scan (1609) was after the cessation of organized updrafts and deviate motion. Comparing the echoes from the four separate spiral scans indicates that the radar top and reflectivity factors were greatest during the most severe stage. The areal extent of the echo was rather constant during all stages with a width of ~15 km.

An inspection of the echo pattern from the first spiral scan (1333) indicates an absence of steep horizontal reflectivity gradients or "echo wall" and an absence of an "overhang" either downwind or on the right flank.

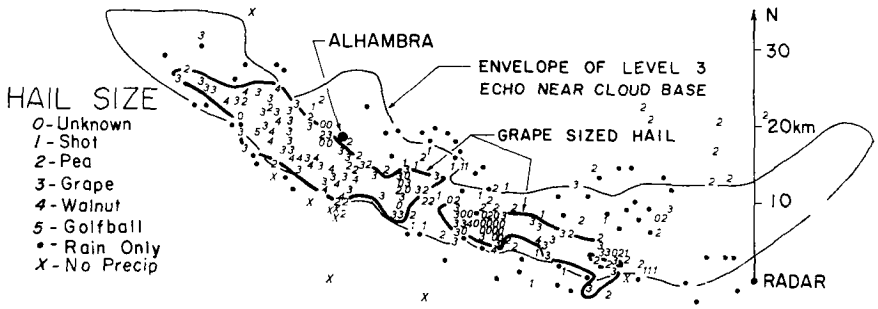

FIG. 4. Hailfall pattern of largest hail sizes from the Alhambra storm.

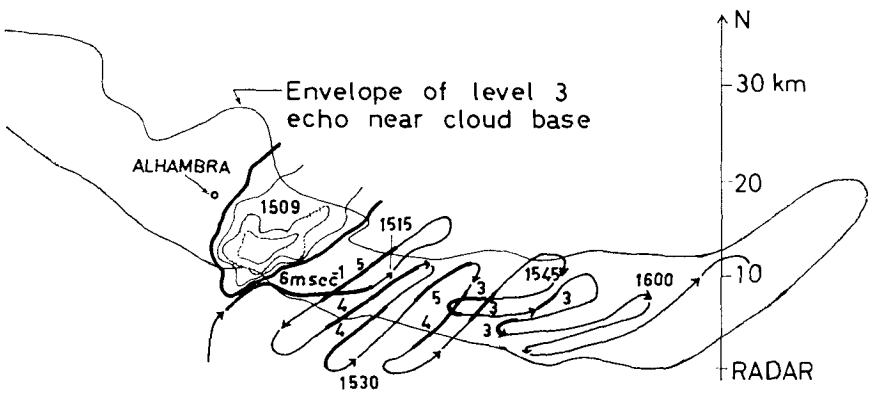

FIG. 5. Flight track of University of Wyoming aircraft and observed updrafts for the Alhambra storm.

There appears to be a bit of an overhang (~2 km) on the west side. No explanation is available for the upwind overhang.

During the severe stage and while organized updrafts were observed (1433 and 1509 in Fig. 6), a distinct echo wall occurred on the southeast side of the echo. An overhang was observed above 5 km and above this echo wall. The overhang extended toward the southeast and over the cloud base updrafts. The direction toward which the overhang was located was such that it could not have been caused by environmental shear tilting the echo downwind (see Figs. 3 and 6).

When the storm was over Alhambra, the aircraft was just north of ALHAS and approaching the storm. At 1448 the air crew took a photograph looking toward 288° from a distance of 60 km (see Fig. 7). The sky was clear and an extensive cloud shield extended ~100 km NE of the storm. A new turret was developing on the southeast side of this storm at the time of the photograph. It should be noted that no precipitation appears to be falling from the new turret at this time. The aircraft arrived at the storm 15 min later and began observing updrafts. The region on the southeast side of the precipitation curtain was observed to be an organized updraft region with peak speeds of 6 m sec^{-1}.

We have already noted from Fig. 2 that the echo patterns at cloud base did not indicate any individual reflectivity cores but appeared to be one large continuous echo. Examination of all of the available echo

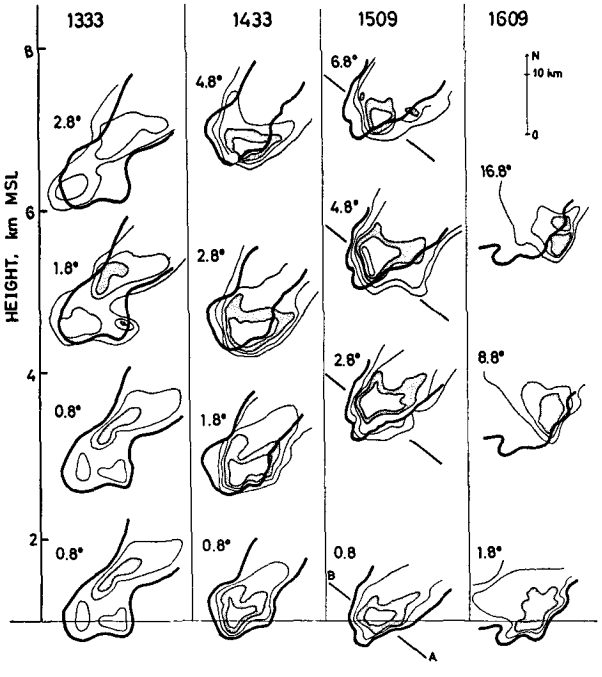

FIG. 6. PPI echoes from the spiral scans at 1333, 1433, 1509 and 1609 for the Alhambra storm. Contours are at 10-dB intervals with the outer edge of the shaded contours corresponding to 41 dBZ (1333), 38 dBZ (1433), 35 dBZ (1509) and 26 dBZ (1609). Outline of echo near cloud base height (thick line) is a fiducial mark.

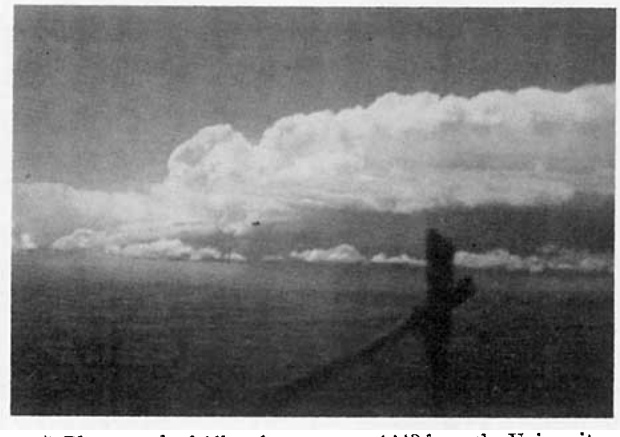

FIG. 7. Photograph of Alhambra storm at 1448 from the University of Wyoming aircraft while approaching the Alhambra storm.

patterns at cloud base of this storm did not reveal any indication of a separate turret developing and merging with the main storm as suggested by the Fig. 7 cloud photo. Echo outlines within 1° of the echo top of the storm are presented at 12-min intervals in Fig. 8. Note that near the time of the photograph (1448, Fig. 7) a new cell was forming and the old one began dissipating. From this figure it is obvious that not only were individual cells propagating to the right of the environmental winds, but discrete propagation was also occurring on the right flank at rather irregular intervals.

At 1505 a packet of 10-cm chaff was released ~4 km ahead of the precipitation curtain. The cloud base updrafts were estimated at 4 m sec^{-1}. Radar signals from the chaff were lost in the storm echo during the third spiral scan. A vertical section was constructed through the chaff track and along the direction of motion of the storm (see Fig. 9). In addition to the radar echo and chaff track, the visual appearance of the precipitation curtain, the region of organized updrafts at cloud base, and the visual boundary of the cloud are included in this figure. It may be noted that the echo overhang extended ~10 km ahead of the precipitation at the surface and ~5 km ahead of the cloud base updrafts. If we define a weak echo region to be a region of strong updrafts containing an echo with a reflectivity factor <10 dBZ, then we observe that this storm did

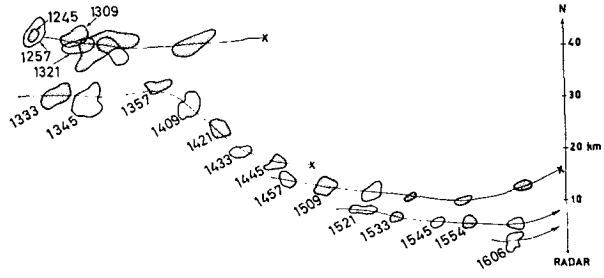

FIG. 8. Echo outlines of individual cells near the top of the Alhambra storm.

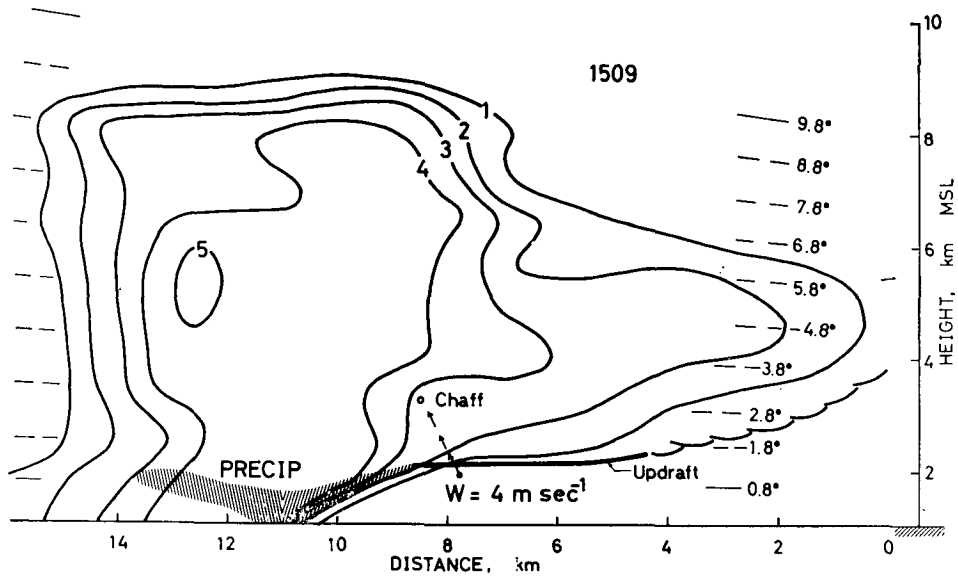

FIG. 9. Vertical section along direction of storm motion at 1509 constructed through chaff trajectory at 1505. Echo patterns are at 10-dB intervals with level three corresponding to 35 dBZ.

not contain a WER since the echo began directly above the updrafts at cloud base.

The fact that the chaff had a velocity with respect to the ground was from 085° at 4 m sec^{-1}, while the storm was moving in nearly the opposite direction (300° at 9 m sec^{-1}), is most remarkable. This means that the warm moist inflow air on which the storm was feeding had a horizontal momentum vector which was substantial and opposite in direction to the storm's motion. Although this is a good indication of propagation, there simply were not enough data to quantify the magnitude and direction of the propagation based on one chaff track for 3 min.

The environmental sounding obtained from Penhold at 1545 is shown in Fig. 10. Parcel theory indicates a thermal buoyancy at 500 mb of 2–3C based on the observed cloud base height and temperature.

From the case study of the Alhambra storm, we have observed a multi-cell storm which deviated to the right of the environmental winds due to discrete propagation on the right flank *plus* continuous propagation of individual cells. Another type of multi-cell storm will now be examined.

4. The Rimbey storm of 16 July 1969

Several rain showers developed during the afternoon of 16 July 1969. Most of the storms, as observed by radar and visual observations, did not appear to be particularly severe. At 1529 the aircraft departed from Penhold in order to observe a line of cells ~50 km NW of the radar near Rimbey.

The PPI echoes from nearest cloud base of the Rimbey storm are presented in Fig. 11 at 30-min intervals. It may be noted that the cells were aligned along an east-west line. The reflectivity cores were located at 3-min intervals from the radar film. Their trajectories are sketched on this figure with their locations noted at 15-min intervals. The reflectivity cores (which are assumed to be individual cells) were found to move from ~195° at 9 m sec^{-1}, while the storm complex had a direction of motion from 235° at 11 m sec^{-1}. It was also noted that cells on the western end of the line of cells were dissipating while new cells were developing at irregular intervals on the eastern or right flank. The cells on the right flank were the most intense.

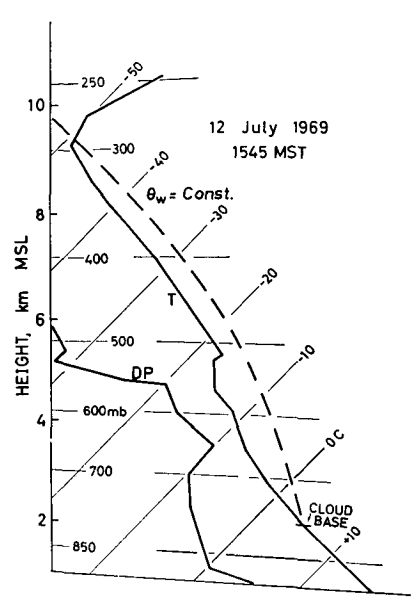

FIG. 10. Penhold sounding of temperature and dew point at 1545.

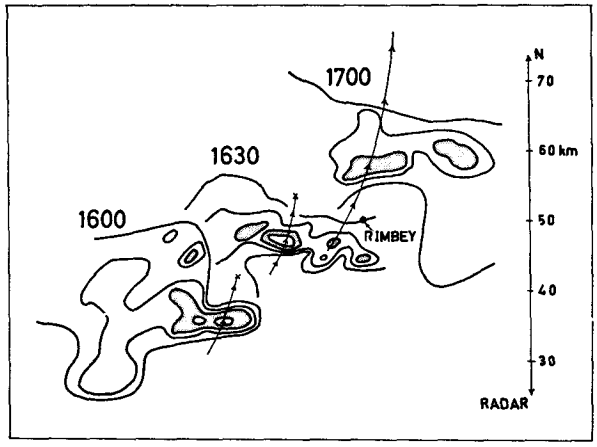

FIG. 11. Echo patterns near height of cloud base for the Rimbey storm of 16 July 1969. The outer edge of the shaded contour is level three, corresponding to 30 dBZ at 37 km.

The aircraft encountered some pea-sized hailstones at 1631 while skirting the eastern end of this line. An area of organized updrafts was located to the north of this line of cells with peak values from 4–6 m sec^{-1} (see Fig. 12). The updrafts were systematically observed for ~50 min. During this time the updrafts persisted and moved from 205° at 12 m sec^{-1}.

The echoes from two spiral scans are presented in Fig. 13. The first spiral scan was taken at 1624, just prior to the arrival of the aircraft; the second scan was taken at 1648, when the third pass was being made by the aircraft. It should be noted at both times that the tops of the individual reflectivity cores were tilted from ~180°. We shall see later that all winds in the cloud layer were from 235–250°. By our empirical rules for locating updrafts, using radar and rawinsonde data on this type of storm (Marwitz *et al.*, 1972), updrafts should be expected on the north side of this line of echoes. The updrafts (with respect to the cloud base PPI echo) are shown on the echoes from the 1648 spiral scan.

During the period when the University of Wyoming aircraft was observing organized updrafts, an echo overhang persisted over the updrafts, i.e., to the north

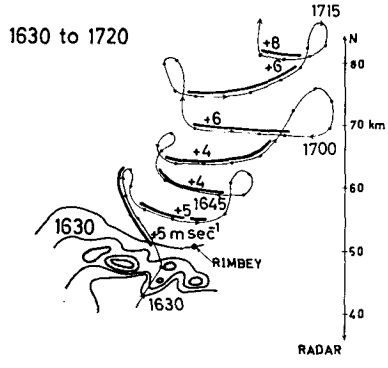

FIG. 12. Flight track of the University of Wyoming aircraft and observed updrafts for the Rimbey storm.

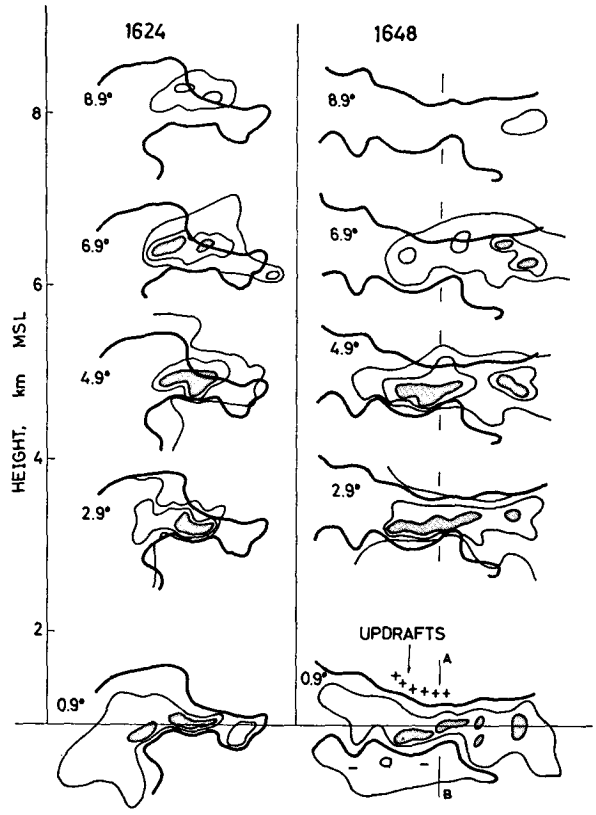

FIG. 13. PPI echoes from the spiral scans at 1624 and 1648 for the Rimbey storm. Contours are at 10-dB intervals with the outer edge of the shaded contour corresponding to 33 dBZ (1624) and 34 dBZ (1648).

of the cloud base echo. The overhang extended 3–4 km north of the cloud base echo.

While the University of Wyoming aircraft was being flown on this storm, an echo wall was not evident on the north side, although a rather steep reflectivity gradient persisted below 5 km along the *south* side of the storm. From 1645–1715 the B-26 aircraft of the University of

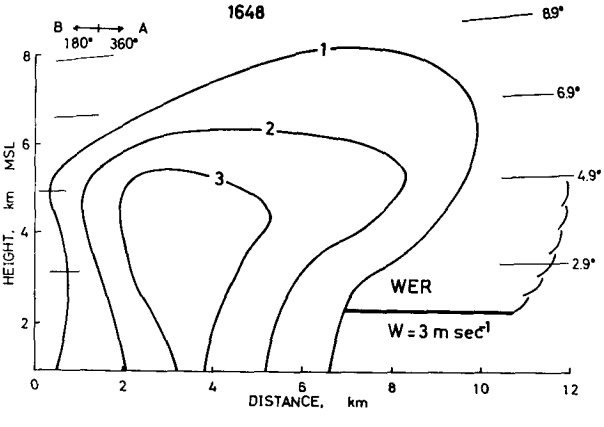

FIG. 14. Vertical section of the Rimbey storm along AB (see Fig. 13) at 1648. Echo patterns are at 10-dB intervals with level three corresponding to 34 dBZ.

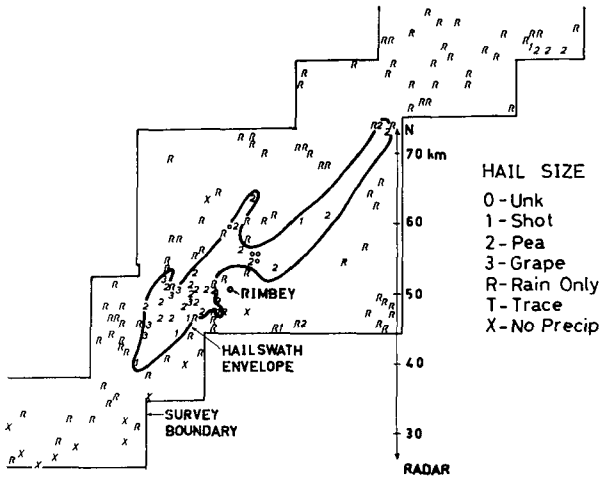

FIG. 15. Hailfall pattern from largest hail sizes for the Rimbey storm.

Nevada (Marwitz and Berry, 1970) was flying near the south side of this storm and encountered no detectable updrafts.

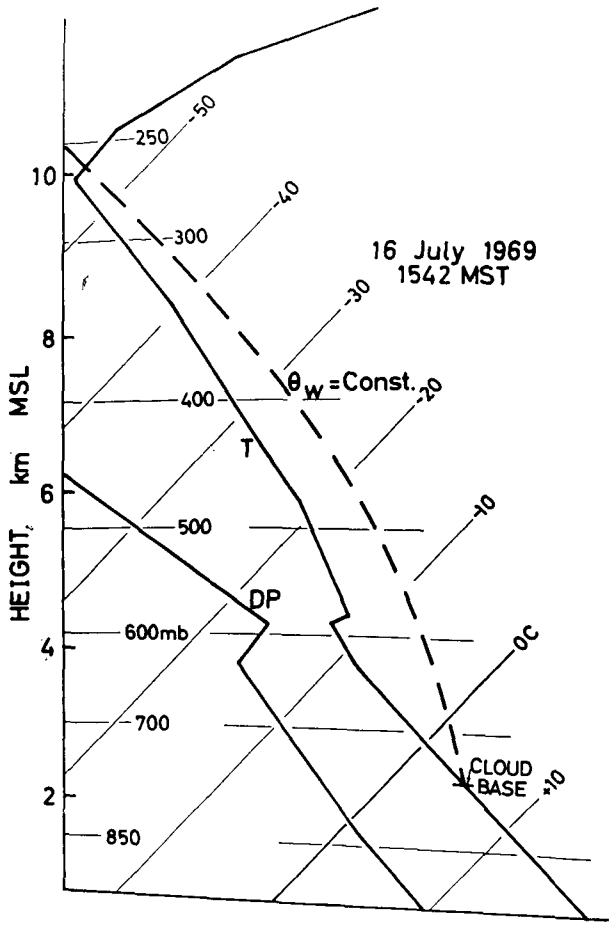

FIG. 16. Edmonton sounding of temperature and dew point at 1542.

Fig. 14 is a vertical section, constructed along the plane AB (1648, Fig. 13), of the precipitation, cloud base and lower visual boundary of the storm. The echo overhang above the organized cloud base updrafts and WER are readily apparent. The above results indicate that strong horizontal reflectivity gradients (i.e., echo walls) do not necessarily indicate the presence of updrafts. The results rather indicate that overhangs and the direction of tilt of reflectivity cores are indicative of the presence of updrafts.

The hailfall data are presented in Fig. 15. Most of the hailstones were pea size with a few reports of grape size for ~15 min, placing this storm just at the lowest threshold of being considered a "severe" storm.

The hailswath moved with the storm's motion but small "hailstreaks" (Changnon, 1970) appear to be superimposed upon the hailswath. The individual echo tracks of Fig. 11 were superimposed upon the hailfall pattern of Fig. 15 and revealed a reasonable correspondence between hailstreaks and individual echoes. It was therefore concluded that the individual cells of this storm were producing the hailstreaks in the hailfall pattern.

The Edmonton temperature and dew point soundings at 1542 are shown in Fig. 16. The cloud base height and temperature were observed by the aircraft system. If the air ascends moist adiabatically within the WER, it would have had ~4C of buoyancy at 500 mb.

The wind hodograph from the above sounding is presented in Fig. 17. The environmental winds were quite weak on this day with values at 10 km reaching only 20 m sec^{-1}. The vertical wind shear through the cloud layer was 2.0×10^{-3} sec^{-1}. The important point to note from this figure is the relationship between the environmental winds and the motions of the cells, updrafts and storm complex. The individual cells making up the storm complex moved to the *left* of the environmental winds while the storm moved *with* the environmental winds. The updrafts and hailstreaks also moved to the left of the environmental winds. It was therefore inferred that individual cells were to be continuously propagating to the left of the environmental winds, while new cell development on the right flank and dissipation of old cells on the left flank were causing discrete propagation to the right. The continuous propagation of the individual cells to the left of the environmental winds was offset by the discrete

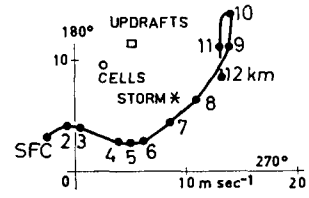

FIG. 17. Hodograph of Edmonton rawinsonde winds for 16 July 1969. Storm, echo and updraft motions are also included.

TABLE 1. Thermodynamic stability and wind shear parameters for certain well-documented multi-cell storms.

Case study	ΔT_{500} (°C)	Veering in sub-cloud (deg)	Mean wind in subcloud (deg/ m sec^{-1})	Mean wind from surface to 10 km (deg/ m sec^{-1})	Storm motion (deg/ m sec^{-1})	Shear in cloud layer (sec^{-1})	Propagation Individual cells	Propagation Discrete
Browning and Ludlam (1960)	+1	160	150/08	210/21	225/18	2.5×10^{-3}	No Propagation	Right
Chrisholm (1966) 18 July 1964	+4	40	240/07	235/26	250/12	—	No Propagation	Right
Chisholm (1966) 21 July 1964	+4	−90	250/06	230/17	250/10	—	No Propagation	Right
Alhambra storm 12 July 1969	+2	30	020/30	245/11	300/09	2.0	Right	Right
Rimbey storm 16 July 1969	+4	30	150/04	240/11	240/11	2.0	Left	Right
Benalto storm 17 July 1968	+3	45	150/04	265/07	305/09	1.5	Right	Right
Sylvan lake storm* 25 July 1968	+6	80	010/04	275/13	315/16	2.0	Right	Right
Carstairs storm 17 July 1969	+4	120	250/03	265/15	295/12	4.0	Right	Right
Butte storm 11 July 1970	+7	10	140/06	235/16	310/07	4.5	Right	Right

* This storm has been synthesized in detail by Chisholm (1970).

propagation to the right. The resultant direction of motion of the storm complex was *along* the mean winds.

5. Summary of environmental conditions surrounding multi-cell storms

It was noted in the Introduction that of the eight Alberta storms which were synthesized, six were of the multi-cell type. The environmental conditions which surrounded the six Alberta storms, as well as those pertaining to the Wokingham storm described by Browning and Ludlam (1960) and that described by Chisholm (1966), are summarized in Table 1. It may be noted in these cases that the range of values for every parameter except one encompassed those of the supercell storm. The mean wind speed in the subcloud layer for the multi-cell storm was $\leqslant 8$ m sec^{-1}, with the median being 4 m sec^{-1}. By comparison, the range of values of the mean wind speed for the supercell cases was 10–17 m sec^{-1} (Marwitz, 1972).

Although the extreme values for instability (ΔT_{500}) and shear in the cloud layer were comparable for both types of storms, the minimum values were substantially less for the multi-cell storms. It is concluded that the distinguishing characteristic of the environment which produces multi-cell storms is light winds in the subcloud layer.

6. Models of multi-cell storms

Browning and Ludlam (1960) presented an elaborate study of the Wokingham storm which pictured a series of aligned cells individually moving with the mean environmental winds. New cells periodically developed on the right flank, moved through the storm complex, and dissipated on the left flank. All deviate motion of the storm complex was due to discrete propagation. Two case studies of Alberta storms were presented which

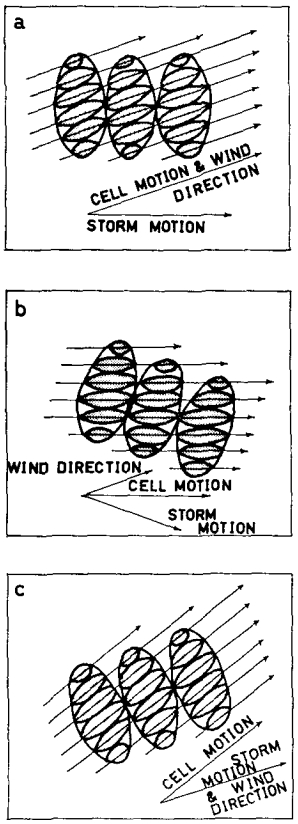

FIG. 18. Schematic diagrams of the Wokingham, Alhambra and Rimbey storms.

displayed two additional modes of propagation of multi-cell storms, i.e., discrete propagation occurred on the right flank of both storms. The individual cells of the Alhambra storm (12 July 1969) propagated continuously to the right, which caused the Alhambra storm to deviate ~55° to the *right* of the mean environmental winds. For the Rimbey storm (16 July 1969), on the other hand, the individual cells were observed to propagate continuously to the *left* of the mean environmental winds. The discrete propagation was acting to cause the storm complex to have a deviate motion to the *right* of the mean environmental winds while the continuous propagation of the cells was acting to the left (see Fig. 11). The storm complex had *no* deviate motion, i.e., it moved in the direction of the mean environmental winds (see Fig. 17). The continuous propagation of the cells was offset by the discrete propagation. Schematic models of the Wokingham, Alhambra and Rimbey storms are shown in Fig. 18.

Acknowledgments. See acknowledgments at end of Part III.

REFERENCES

Browning K. A., and F. H. Ludlam, 1960: Radar analysis of a hailstorm. Tech. Note No. 5, Contract AF61(052)-254, Dept. of Meteorology, Imperial College, London, 109 pp.

——, and ——, 1962: Airflow in convective storms. *Quart. J. Roy. Meteor. Soc.*, **88**, 117–135.

Changnon, Jr., S. A., 1970: Hailstreaks. *J. Atmos. Sci.*, **27**, 109–125.

Chisholm, A. L., 1966: Small-scale structure of Alberta hailstorms. M.Sc. thesis, Dept. of Meteorology, McGill University, Montreal, 73 pp.

Dennis, A. S., C. A. Schock and A. Koscielski, 1970: Characteristics of hailstorms of western South Dakota. *J. Appl. Meteor.*, **9**, 127–135.

Fankhauser, J. C., 1967: Some physical and dynamical aspects of a severe right moving cumulonimbus. Tech. Memo No. 32, National Severe Storms Lab., Norman, Okla., 11–32.

Marwitz, J. D., and E. X Berry, 1970: The weak echo region and updrafts of a severe hailstorm. *Preprints of Papers, Fourteenth Radar Meteor. Conf.*, Tucson, Ariz., Amer. Meteor. Soc., 43–47.

——, 1972: The structure and motion of severe hailstorms, Part I. Supercell storms, *J. Appl. Meteor.*, **11**, 166–179.

——, A. H. Auer, Jr., and D. L. Veal, 1972: Locating the organized updraft on severe thunderstorms. *J. Appl. Meteor.*, **11**, 236–238.